AIP Applied Physics Letters

Effect of Ti doping concentration on resistive switching behaviors of Yb2O3 memory cell

Somnath Mondal, Hung-Yu Chen, Jim-Long Her, Fu-Hsiang Ko, and Tung-Ming Pan

Citation: Applied Physics Letters **101**, 083506 (2012); doi: 10.1063/1.4747695
View online: http://dx.doi.org/10.1063/1.4747695
View Table of Contents: http://scitation.aip.org/content/aip/journal/apl/101/8?ver=pdfcov
Published by the AIP Publishing

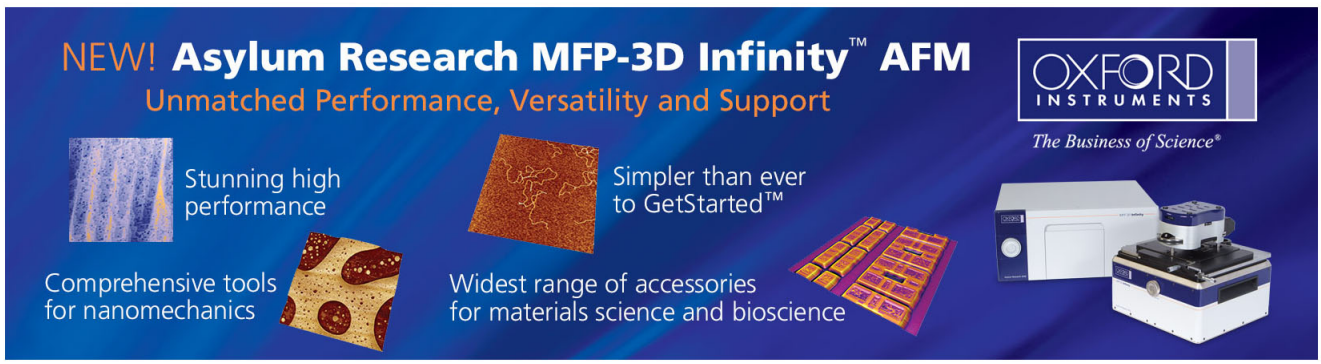

Effect of Ti doping concentration on resistive switching behaviors of Yb_2O_3 memory cell

Somnath Mondal,[1] Hung-Yu Chen,[1] Jim-Long Her,[2] Fu-Hsiang Ko,[3] and Tung-Ming Pan[1,a)]
[1]*Department of Electronics Engineering, Chang Gung University, Taoyuan 333, Taiwan*
[2]*Division of Natural Science, Center for General Education, Chang Gung University, Taoyuan 333, Taiwan*
[3]*Department of Materials Science and Engineering, Institute of Biological Science and Technology, National Chiao-Tung University, Hsinchu 300, Taiwan*

(Received 6 July 2012; accepted 8 August 2012; published online 23 August 2012)

We investigate the resistive memory switching behaviors of Yb_2O_3 thin films for different Ti-dopant concentrations. A higher doping concentration of 9.4% of Ti atom into Yb_2O_3 thin film causes the switching mechanism to change from bipolar to unipolar behavior. This is ascribed to different chemical compositions of the filament through the oxide film. The reset mechanism is associated with the annihilation of oxygen vacancies and other ionic and electronic defects within or near the interface area of oxide film for bipolar switching, while it is believed to be due to rupture of the conducting filament by local Joule heating effect for unipolar resistive switching. Furthermore, the incorporation of Ti atom into the Yb_2O_3 memory device exhibits improved electrical performances including low set/reset voltages and good endurance and retention characteristics. © *2012 American Institute of Physics*. [http://dx.doi.org/10.1063/1.4747695]

Resistive random access memory (ReRAM) is an emerging storage device for future nonvolatile memory applications because of its simple design, excellent scalability, high switching speed, and compatibility with complementary metal–oxide–semiconductor process.[1–7] Based on the electrical field induced change of resistivity in some metal oxides, ReRAM devices switch between two different resistance states namely a high-resistance state (HRS) and a low-resistance state (LRS). A variety of metal oxides, including TiO_2, HfO_2, Al_2O_3, ZrO_2, and Yb_2O_3,[8–12] have widely been investigated for ReRAM device applications. Although resistance-switching phenomena in several binary metal oxides have been known from decades, the details of the switching mechanisms and the nature of the different resistive states are still under debate. However, two dominant resistive switching mechanisms have been classified into the "interface type" and "filament type" to clarify the driving mechanism of resistive switching. The application of Yb_2O_3 thin film in ReRAM device had testified and demonstrated the formation and rupture of filamentary path in resistive switching.[12] In order to use the Yb_2O_3-based ReRAM for the practical implementation, its switching behavior needs to be fully controlled. The stochastic formation and rupture of the filaments are one of the major challenges that need to be minimized to improve the stability of resistive switching characteristics. So far, one approach of negative bias stress after a standard forming process has been demonstrated to improve the resistive switching in Yb_2O_3 thin film.[12]

In this study, we explored the influence of Ti doping concentration on the resistive switching characteristics of Yb_2O_3-based ReRAM device. It has been reported that the doping of Ti stabilizes the resistive switching behavior in the memory device.[13,14] The Ti-doped Yb_2O_3 ReRAM devices exhibit excellent switching characteristics with reliable switching endurance and data retention suitable for future nonvolatile memory applications. Besides, our works focus on the driving mechanism of resistive switching of the memory cell with different Ti-dopant concentrations. The switching behavior changes from bipolar to unipolar resistive switching with increasing doping concentration of Ti atom (above 5%) into the Yb_2O_3 film. A plausible mechanism is proposed to explain the influence of Ti doping on resistive switching behaviors of Yb_2O_3-based ReRAM devices.

The TaN bottom electrode was deposited on SiO_2/Si wafer substrates by dc sputter deposition technique. A 30-nm Ti doped Yb_2O_3 (Ti:Yb_2O_3) film with different Ti atomic concentrations was deposited on the TaN electrode through reactive rf sputtering from both Yb and Ti targets at room temperature.[15] The chamber working pressure was maintained at 10 mTorr, and the Ar/O_2 flow was set at 3/1. The atomic concentration of the Ti dopant was examined by Auger electron spectroscopy (AES) analysis on the ReRAM devices. The AES analysis was performed on the selected devices at LRS condition after 10 resistive switching cycles. The physical thickness and film behaviors of the oxide layer were confirmed by cross-section transmission electron microscopy (TEM) image (not shown here). The chemical bonding of the oxide films was analyzed by x-ray photoelectron spectroscopy (XPS). Finally, a 100-nm Ni top electrode was deposited on the oxide film through shadow mask by thermal evaporation technique. The electrical measurements were performed in semi-automated cascade system using Agilent E5260A high speed semiconductor parameter analyzer.

To investigate the structural and compositional changes of the Ti doped Yb_2O_3 thin films with different Ti doping concentrations, AES and XPS analyses were performed. Fig. 1(a) shows the AES analysis data of the Ni/Ti:Yb_2O_3/TaN devices for different Ti atomic concentrations of 3.5%, 5.0%, and 9.4%. Fig. 1(b) displays the O 1s spectra, with appropriate curve-fitting of peaks, for different Ti doping

a)E-mail: tmpan@mail.cgu.edu.tw. Tel.: 886-3-211-8800. Fax: 886-3-211-8507.

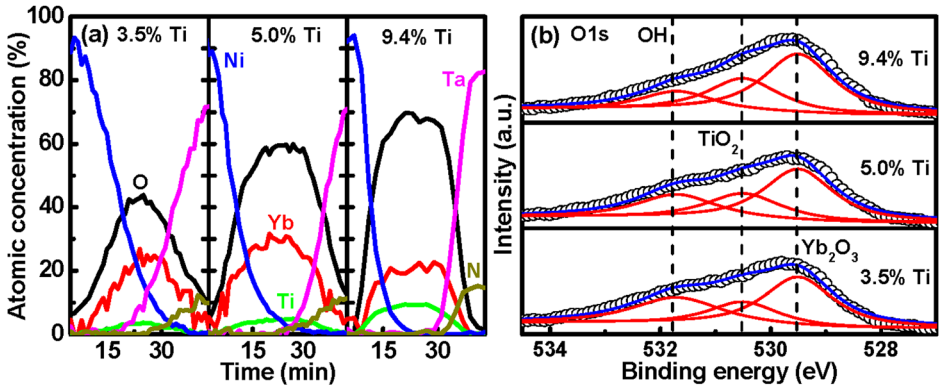

FIG. 1. (a) AES depth-profiling analysis of the Ni/Ti:Yb_2O_3/TaN interface with different Ti concentrations. (b) XPS line-shape analysis of O 1s spectra for the Ni/Ti:Yb_2O_3/TaN memory devices with different Ti concentrations.

concentrations in the Yb_2O_3 film. Adventitious hydrocarbon C 1s binding energy at 285 eV was used as a reference to correct the energy shift of O 1s core levels due to differential charging phenomena. Each fitting peak followed the general shape of the Lorentzian–Gaussian function. In the three sets of spectra, the O 1s peaks at 529.5, 530.5, and 531.7 eV represent the Yb–O,[16] Ti–O,[17] and OH (Refs. 18 and 19) bonds, respectively. The intensity of O 1s peak corresponding to OH bond decreases with increasing the Ti doping concentration, while the intensity of O 1s peak corresponding to TiO_2 increases accordingly. The high Ti content in Yb_2O_3 film effectively decreases the nonlattice oxygen ions from the oxide film.

Figure 2(a) shows the electro-forming process of the Yb_2O_3 (0% Ti) and Ti:Yb_2O_3 (3.5% Ti and 5.0% Ti) memory devices with a current compliance of 100 μA. The Ti-doped Yb_2O_3 memory device exhibited a lower forming voltage than the Yb_2O_3 memory device. The lower forming voltage can be attributed to the easy formation of the field induced oxide defects into the Yb_2O_3 film due to lower formation energy of the Ti-O compound.[14] After a standard electro-forming process, typical bipolar resistive switching characteristics of the Ti:Yb_2O_3 (3.5% Ti and 5.0% Ti) memory devices are shown in Figs. 2(b) and 2(c), respectively. During set process in Ni/Ti:Yb_2O_3/TaN with Ti atomic concentration of 3.5% and 5.0%, a negative dc bias sweep with a current compliance of $\leq$1 mA causes the device suddenly transformed from HRS to LRS. The high current during set operation is guided by the broken filamentary path in the oxide, which can overwhelm the uncontrollable breakdown of the oxide thin film. In a subsequent positive sweep in reset process, the device can be switched again to HRS and a bipolar resistive switching is achieved. In contrary, Fig. 2(d) exhibits the unipolar resistive switching behavior of the memory device with Ti atomic concentration of 9.4% in positive bias sweep without any electroforming process. A stable and reproducible resistive memory switching can be performed more than 1000 sweeping cycles in the Ti:Yb_2O_3 (5.0% Ti and 9.4% Ti) memory devices, while a failure from LRS to HRS transition after few cycles occurs for device with a low Ti content (3.5% Ti) or no Ti doping concentration (not shown).

The driving mechanism of the resistive switching characteristics in Ti:Yb_2O_3 thin film with different Ti doping concentrations was investigated. The HRS and LRS resistance values as a function of the device size for Ti:Yb_2O_3

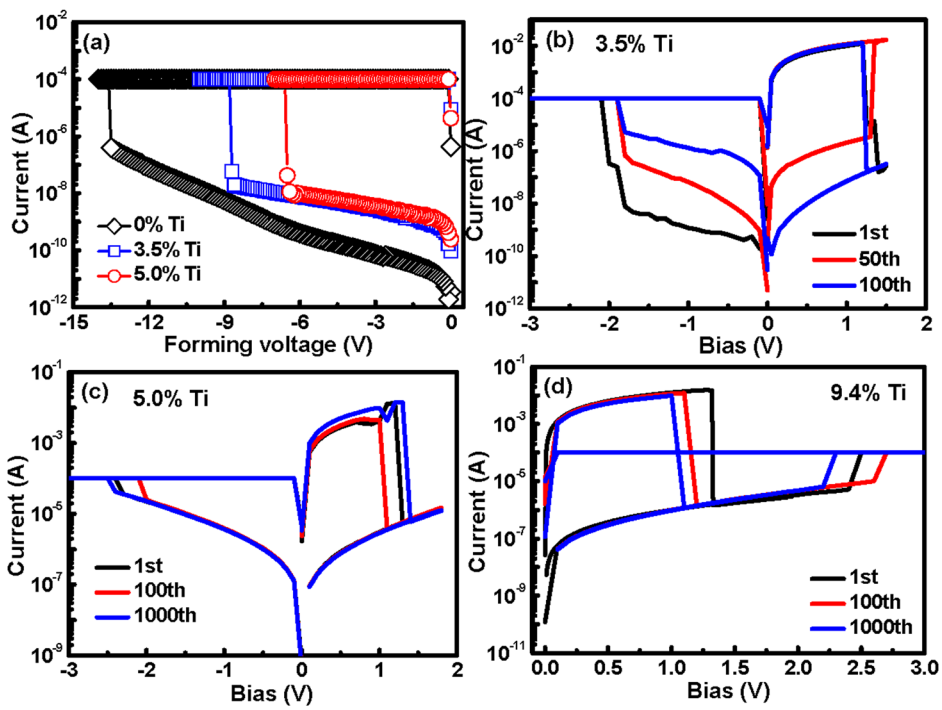

FIG. 2. (a) Electro-forming process in the Yb_2O_3 and Ti:Yb_2O_3 memory devices for different Ti atomic concentrations. Reproducible resistive switching behavior of the ReRAM cells with different Ti doping concentrations (b) 3.5%, (c) 5.0%, and (d) 9.4%.

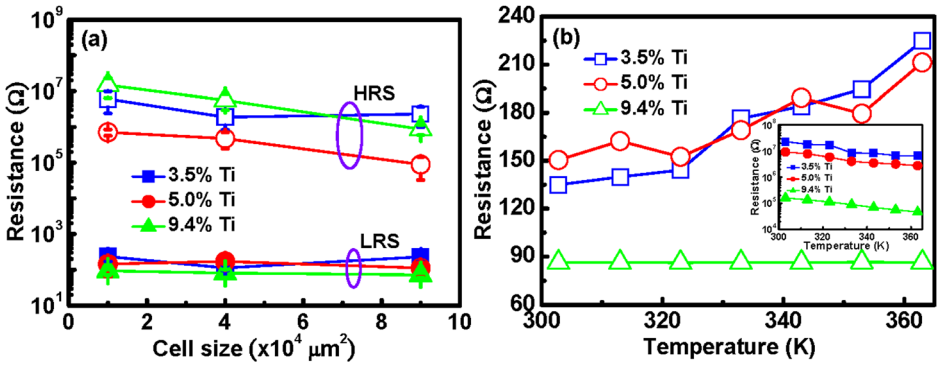

FIG. 3. (a) Device size dependence HRS and LRS values of Ni/Ti:Yb_2O_3/TaN memory devices for different Ti concentrations. (b) Temperature dependence LRS value of Ni/Ti:Yb_2O_3/TaN memory cells for different Ti concentrations. Inset: temperature dependence HRS value of Ni/Ti:Yb_2O_3/TaN memory cells for different Ti concentrations. The LRS and HRS values of the memory devices with 5% Ti and 3.5% Ti concentrations were measured in bipolar mode, whereas the device with 9.4% Ti was tested in unipolar mode.

memory devices with different Ti concentrations are plotted in Fig. 3(a). The LRS values of the Ti:Yb_2O_3 memory devices seem to be insensitive to the cell size. Therefore, the formation and rupture of percolated filamentary paths by oxygen vacancies or metal ions/defects are preferred as the driving mechanism of resistive switching.[20] We consider that the percolation of localized filament in the devices is associated with the oxygen vacancies and other ionic and electronic defects within or near the interface area for bipolar resistive switching, while it is accompanying with the oxygen migration between two metal electrodes for unipolar resistive switching behavior. During set process in bipolar resistive switching, the large number of nonlattice oxygen ions and oxide defects drift towards opposite polarity of electrode making a conducting filament into the oxide thin films. The devices transform from HRS to LRS. The oxygen ions are absorbed by the anode (TaN) to form a very thin conducting interfacial layer which, acts as oxygen reservoir[21] and/or modifies the electrical contact of the interface.[13] By applying opposite polarity bias of set process, the absorbed oxygen ions are released from the oxide/anode interface causing the rupture of conducting filament and the devices switches from LRS to HRS. Fig. 3(b) shows the temperature dependence resistance in LRS for memory devices with different Ti concentrations. For lower Ti atomic concentration ($\leq$5% Ti), the LRS increases with increasing the temperature, indicating the formation of metallic filament by percolation of oxygen vacancies and other ionic and electronic defects within or near the interface area.[12] The unipolar resistive switching behavior in device with higher Ti atomic concentration (>5% Ti) can be attributed to formation and rupture of filament by oxygen migration between two metal electrodes and Joule heating effect, respectively. It has been reported that Ni as one of the electrodes in some oxide systems shows unipolar resistive switching behavior because of the diffusion of Ni ions during electroforming process into the oxide film.[22,23] The Ni/Ti:Yb_2O_3/TaN memory cell with 9.4% Ti atomic concentration shows no Ni diffusion during resistive switching as evidenced by AES spectra in Fig. 1(a). This may be due to the fact that the formation of unipolar resistive switching behavior of the Ti:Yb_2O_3 film is not related to Ni ions in the memory device. By applying a predefined set voltage on the Ti:Yb_2O_3 (9.4% Ti) memory device, the electrical fields induced mobile oxygen ions are generated accompanying with oxygen vacancies in the oxide and, thus, propagate through the oxide until conducting filaments formed in the oxide film. These mobile oxygen ions are chemisorbed at the grain boundary or penetrate through the Ni electrode. The resistance value of LRS in unipolar memory device (9.4% Ti) remained almost unchanged upon increasing temperature, as shown in Fig. 3(b). The semiconducting behavior of the LRS conduction process corroborates well with the filament formation mechanism by field induced oxygen vacancies in the oxide film.[12] The transition from LRS to HRS is believed to be related to the rupture of the conducting filament by local Joule heating. The temperature dependence HRS is shown in the inset of Fig. 3(b). The HRS resistance decreases with increasing temperature, indicating oxide or semiconducting conduction mechanism in the memory devices. Furthermore, the bipolar memory devices (3.5% Ti and 5.0% Ti) exhibit a higher value of LRS than the unipolar memory device (9.4% Ti). This may be due to the formation of interfacial layer by absorbed oxygen ions at the oxide/TaN interface, which acts as a series resistance to the LRS value.[24]

Significant changes of the resistive switching behaviors are observed with increasing Ti atomic concentration into Yb_2O_3 thin film. The set/reset voltages of the Ti-doped Yb_2O_3 memory devices are shown in Fig. 4. The reset voltages decrease gradually with increasing Ti atomic concentration in the Ni/Ti:Yb_2O_3/TaN memory devices. Moreover, the devices exhibit more stable switching in set/reset process with higher Ti atomic concentration and the distribution of set/reset voltages decreases significantly. The lower enthalpy of the Ti-O compound may induce the oxygen vacancies (Yb^0) and compensate the defects in the oxide, which effectively improve the set/reset voltages of the device.[10,14,15]

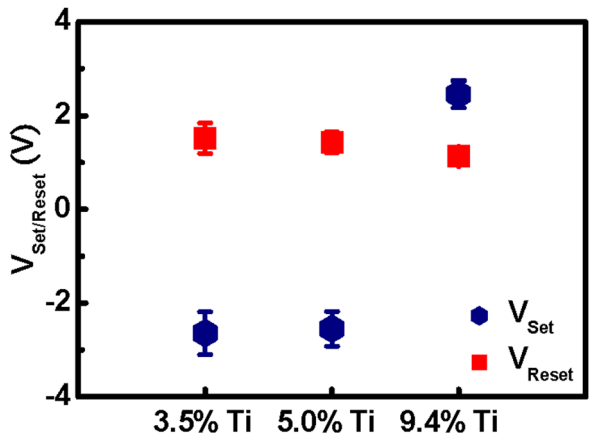

FIG. 4. Set/reset voltage distribution of the Ni/Ti:Yb_2O_3/TaN memory devices for different Ti concentrations.

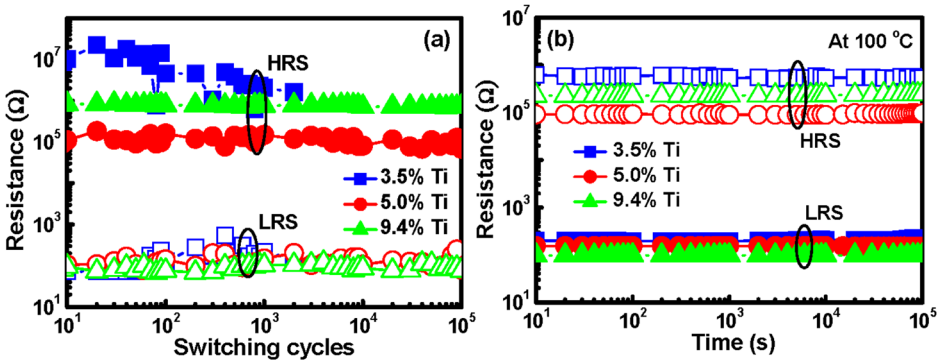

FIG. 5. (a) Pulse induced resistive switching endurance characteristics of the Ni/Ti:Yb_2O_3/TaN memory devices for different Ti concentrations. (b) Retention behavior of the Ni/Ti:Yb_2O_3/TaN memory cells for different Ti concentrations measured at 100 °C.

To consider the Ni/Ti:Yb_2O_3/TaN devices for ReRAM applications, endurance and retention tests of the devices were performed. Fig. 5(a) illustrates the endurance characteristics of the Ni/Ti:Yb_2O_3/TaN devices under pulse voltages for different Ti doping concentrations. Both bipolar and unipolar resistive switching devices can be switched over 10^5 cycles with R_{HRS}/R_{LRS} ratio of about 10^3. But, the failure of resistance switching from LRS to HRS happens after few hundreds cycles in the bipolar Ni/Ti:Yb_2O_3/TaN device for 3.5% Ti atomic concentration. We believe that the localized Ti ions in Ti-doped Yb_2O_3 films help to the formation of conducting filaments through the oxide film easily, resulting in an improved resistive switching behavior of the devices.[14] Furthermore, the retention characteristics of all the Ti-doped memory devices after 10^5 switching cycles are shown in Fig. 5(b). No degradation in retention behavior of the memory devices are observed after 10^5 s, measured at 100 °C.

In conclusion, the influence of Ti doping on resistive switching behaviors in Yb_2O_3-based resistive random access memory has been investigated. The resistive switching characteristics of Ni/Ti:Yb_2O_3/TaN memory device depend on the Ti-dopant concentration in oxide film. The resistive switching behavior changes from bipolar to unipolar resistive switching as the Ti atomic concentration in the Ti:Yb_2O_3 film changes to higher value. The driving mechanism of different resistance switching behaviors can be attributed to different chemical compositions of the filament through the oxide. The reset process in the bipolar memory devices is attributed to the annihilation of oxide defects in the oxide film, whereas the disruption of filament through Joule heating effect is responsible for unipolar resistive switching devices. Furthermore, the high Ti content in the Yb_2O_3 memory device exhibits improved electrical performances including reduced set/reset voltage and good endurance and retention characteristics.

This work was supported by the National Science Council (NSC) of Taiwan under Contract No. NSC-98-2221-E-182-056-MY3.

[1]B. J. Choi, D. S. Jeong, S. K. Kim, C. Rohde, S. Choi, J. H. Oh, H. J. Kim, C. S. Hwang, K. Szot, R. Waser, B. Reichenberg, and S. Tiedke, J. Appl. Phys. **98**, 033715 (2005).
[2]T. W. Hickmott, J. Appl. Phys. **33**, 2669 (1962).
[3]K. Szot, W. Speier, R. Carius, U. Zastrow, and W. Beyer, Phys. Rev. Lett. **88**, 75508 (2002).
[4]S. Tsui, A. Baikalov, J. Cmaidalka, Y. Y. Sun, Y. Q. Wang, Y. Y. Xue, C. W. Chu, L. Chen, and A. J. Jacobson, Appl. Phys. Lett. **85**, 317 (2004).
[5]S. Seo, M. J. Lee, D. H. Seo, E. J. Jeoung, D.-S. Suh, Y. S. Joung, I. K. Yoo, I. R. Hwang, S. H. Kim, I. S. Byun, J.-S. Kim, J. S. Choi, and B. H. Park, Appl. Phys. Lett. **85**, 5655 (2004).
[6]S. Zhang, S. Long, W. Guan, Q. Liu, Q. Wang, and M. Liu, J. Phys. D: Appl. Phys. **42**, 055112 (2009).
[7]A. Beck, J. G. Bednorz, Ch. Gerber, C. Rossel, and D. Widmer, Appl. Phys. Lett. **77**, 139 (2000).
[8]K. M. Kim, B. J. Choi, Y. C. Shin, S. Choi, and C. S. Huang, Appl. Phys. Lett. **91**, 012907 (2007).
[9]H. Zhang, L. Liu, B. Gao, Y. Qiu, X. Liu, J. Lu, R. Han, J. Kang, and B. Yu, Appl. Phys. Lett. **98**, 042105 (2011).
[10]Y. Wu, B. Lee, and H.-S. P. Wong, IEEE Electron Device Lett. **31**, 1449 (2010).
[11]Q. Liu, W. Guan, S. Long, R. Jia, and M. Liu, Appl. Phys. Lett. **92**, 012117 (2008).
[12]H.-C. Tseng, T.-C. Chang, J.-J. Huang, P.-C. Yang, Y.-T. Chen, F.-Y. Jian, S. M. Sze, and M.-J. Tsai, Appl. Phys. Lett. **99**, 132104 (2011).
[13]O. Heinonen, M. Siegert, A. Roelofs, A. K. Petford-Long, M. Holt, K. d'Aquila, and W. Li, Appl. Phys. Lett. **96**, 103103 (2010).
[14]Q. Liu, S. Long, W. Wang, Q. Zuo, S. Zhang, J. Chen, and M. Liu, IEEE Electron Device Lett. **30**, 1335 (2009).
[15]S. Mondal, J. L. Her, F. H. Chen, S. J. Shih, and T. M. Pan, IEEE Electron Device Lett. **33**, 1069 (2012).
[16]T.-M. Pan and J.-W. Chen, Appl. Phys. Lett. **93**, 183510 (2008).
[17]B. Erdem, R. A. Hunsicker, G. W. Simmons, E. D. Sudol, V. L. Dimonie, and M. S. El-Aasser, Langmuir **17**, 2664 (2001).
[18]S. Mondal, J.-L. Her, S.-J. Shih, and T.-M. Pan, J. Electrochem. Soc. **159**, H589 (2012).
[19]D. Eom, S. Y. No, H. Park, C. S. Hwang, and H. J. Kim, Electrochem. Solid-State Lett. **10**, G93 (2007).
[20]M.-C. Chen, T.-C. Chang, C.-T. Tsai, S.-Y. Huang, S.-C. Chen, C.-W. Hu, S. M. Sze, and M.-J. Tsai, Appl. Phys. Lett. **96**, 262110 (2010).
[21]C.-Y. Lin, C.-Y. Wu, C.-Y. Wu, T.-Y. Tseng, and C. Hu, J. Appl. Phys. **102**, 094101 (2007).
[22]Y. Y. Chen, G. Pourtois, C. Adelmann, L. Goux, B. Govoreanu, R. Degreave, M. Jurczak, J. A. Kittl, G. Groeseneken, and D. J. Wouters, Appl. Phys. Lett. **100**, 113513 (2012).
[23]T.-H. Hou, K.-L. Lin, J. Shieh, J.-H. Lin, C.-T. Chou, and Y.-J. Lee, Appl. Phys. Lett. **98**, 103511 (2011).
[24]S.-Y. Wang, D.-Y. Lee, T.-Y. Tseng, and C.-Y. Lin, Appl. Phys. Lett. **95**, 112904 (2009).